Biointerphases (2012) 7:7
DOI 10.1007/s13758-011-0007-5

IN FOCUS: NANOMEDICINE - ARTICLE

Design and Preparation of a Nanoprobe for Imaging Inflammation Sites

Toru Yoshitomi · Yukio Nagasaki

Received: 6 September 2011 / Accepted: 22 November 2011 / Published online: 9 February 2012

Abstract To image inflammation sites, we developed a novel nanoparticle, hydroxylamine-containing nanoparticle (HANP), which emits an intense electron spin resonance (ESR)-signal triggered by enzymatic oxidation reaction and pH-sensitive self-disintegration. The nanoparticle was prepared from an amphiphilic block copolymer, poly (ethylene glycol)-*b*-poly[4-(2,2,6,6-tetramethylpiperidine-1-hydroxyl)aminomethylstyrene] (PEG-*b*-PMNT-H), which spontaneously forms a core–shell type polymeric micelle (particle diameter = ca. 50 nm) in aqueous media. Because the PMNT-H segment in the block copolymer possesses amino groups in each repeating unit, the particle can be disintegrated by protonation of the amino groups in an acidic pH environment such as inflammation sites, which is confined to the hydrophobic core of HANP. Mixing HANP with horseradish peroxidase (HRP)/H_2O_2 mixture resulted in enzymatic oxidization of the hydroxylamines in the PEG-*b*-PMNT-H and converted the hydroxylamine to the stable nitroxide radical form in PEG-*b*-poly[4-(2,2,6,6-tetramethylpiperidine-1-oxyl)aminomethylstyrene] (PEG-*b*-PMNT), which shows an intense ESR signal. It is interesting to note that the ESR signal increased at a greater rate under acidic conditions (pH 5.6) than that under neutral conditions (pH 7.4), although the enzymatic activity of HRP under neutral conditions is known to be much higher than that under acidic conditions. This indicates that enzymatic oxidation reaction was accelerated by synchronizing the disintegration of HANP under acidic conditions. On the basis of these results, HANP can be used as a high-performance ESR probe for imaging of inflammation sites.

This article is part of the Topical Collection "In Focus: Nanomedicine".

Electronic supplementary material The online version of this article (doi:10.1007/s13758-011-0007-5) contains supplementary material, which is available to authorized users.

T. Yoshitomi · Y. Nagasaki (✉)
Department of Materials Sciences, Graduate School of Pure and Applied Sciences, University of Tsukuba, Tennoudai 1-1-1, Tsukuba, Ibaraki 305-8573, Japan
e-mail: yukio@nagalabo.jp

Y. Nagasaki
Master's School of Medical Sciences, Graduate School of Comprehensive Human Sciences, University of Tsukuba, Tennoudai 1-1-1, Tsukuba, Ibaraki 305-8573, Japan

Y. Nagasaki
Satellite Laboratory, International Center for Materials Nanoarchitectonics (MANA), National Institute for Materials Science (NIMS), Tennoudai 1-1-1, Tsukuba, Ibaraki 305-8573, Japan

1 Introduction

Inflammation is strongly related to various disorders and diseases such as rheumatoid arthritis, multiple sclerosis, and inflammatory bowel disease [1]. Furthermore, tumors are known to develop at chronic inflammation sites, and inflammatory cells have been shown to be present in biopsied samples from tumors [2, 3]. A non-invasive imaging probe for detecting inflammation at an early and subclinical stage is important not only for decisions related to the necessity of therapy and subsequent prediction of outcomes but also for diagnostics of several diseases including cancer. To image an inflamed area, a probe with a high signal-to-background ratio is desirable. Promising strategies to improve the signal-to-background ratio include "specific accumulation of probe at the inflamed area" and "on–off regulation of signal", in which the imaging probe ideally has no signal in the non-target tissue and is activated at the inflamed area.

Nanoprobes are the candidates for specific accumulation at an inflamed area because they accumulate in inflammation sites due to an increased vascular permeability [4]. Inflammation is a complex cellular event, during which various cytokines are released and excess reactive oxygen species (ROS) are generated by immune cells [5]. Interstitial acidification is commonly associated with the course of inflammatory reactions against pathogenic microorganisms in peripheral tissues, where extracellular pH values as low as 5.5–7.0 have been observed [6–8]. For achieving "on–off regulation" of imaging probes at inflammation sites, nanoparticle-type probes capable of on–off signal regulation in response to an acidic pH and oxidation by ROS are desirable.

Among non-invasive imaging techniques, magnetic resonance imaging (MRI) and electron spin resonance imaging (ESRI) are two of the most powerful tools for visualizing specific and deep tissues. In particular, electron spin resonance (ESR) is highly sensitive [9, 10], and in vivo imaging has been achieved using L-band ESR instruments [11, 12]. Hydroxylamines such as 2,2,6,6-tetramethylpiperidine-1-hydroxyl are the candidates as ROS-sensitive probes and function as ESRI and MRI probes after hydroxylamines are oxidized by superoxide and peroxylnitrite or its decomposition products to corresponding nitroxide radicals, such as 2,2,6,6-tetramethylpiperidine-1-oxyl (TEMPO), with an intense ESR signal [13–15]. If hydroxylamine can accumulate in an inflamed area, it may be useful for imaging of inflammation sites. However, low-molecular-weight hydroxylamines cause several problems such as autoxidation before use, preferential renal clearance, and diffusion throughout the whole body.

We developed a nitroxide radical-containing nanoparticle (RNP) for use as a nanomedicine for oxidative stress injury [16–20] and as a bioimaging nanoprobe for MRI and ESRI [21], which is composed of a poly(ethylene glycol)-*b*-poly(methylstyrene) block copolymer possessing TEMPO moieties via an amine linkage (PEG-*b*-PMNT) [22]. This PEG-*b*-PMNT forms core–shell-type micelles in the physiological environment; the cumulant average diameter of the RNP is about 40 nm, and it emits an intense ESR signal. The toxicity of RNP is extremely low due to the confinement of the 4-amino TEMPO moieties in the hydrophobic core of RNP [21]. The RNP was confirmed to have long-term spin circulation in the blood due to the formation of polymeric micelles in the blood stream. Disintegration of RNP is caused by protonation of the amino groups in response to acidic pH, which typically occurs at inflammation sites, since amino groups are introduced into the hydrophobic segments of amphiphilic block copolymers [17]. Along with the decreasing in pH, ESR signals of RNP gradually change from broad to sharp triplets. On the basis of these changes in ESR signals, we confirmed that phantom images showed remarkable on–off regulation in response to acidic conditions. However, RNP, as an imaging agent, exhibits undesirable background signals due to broad signal of RNP under physiological conditions.

If nanoparticle, that emits a signal following a reaction with ROS in the inflamed area, would be developed, it can be used as a probe for imaging of inflammation sites. To develop such high-performance nanoprobe for imaging of inflammation sites, we designed and developed a pH-sensitive hydroxylamine-containing nanoparticle (HANP), which emits an ESR-signal triggered by an oxidation reaction and pH-sensitive self-disintegration (Fig. 1). Here, we describe the preparation and characterization of HANP.

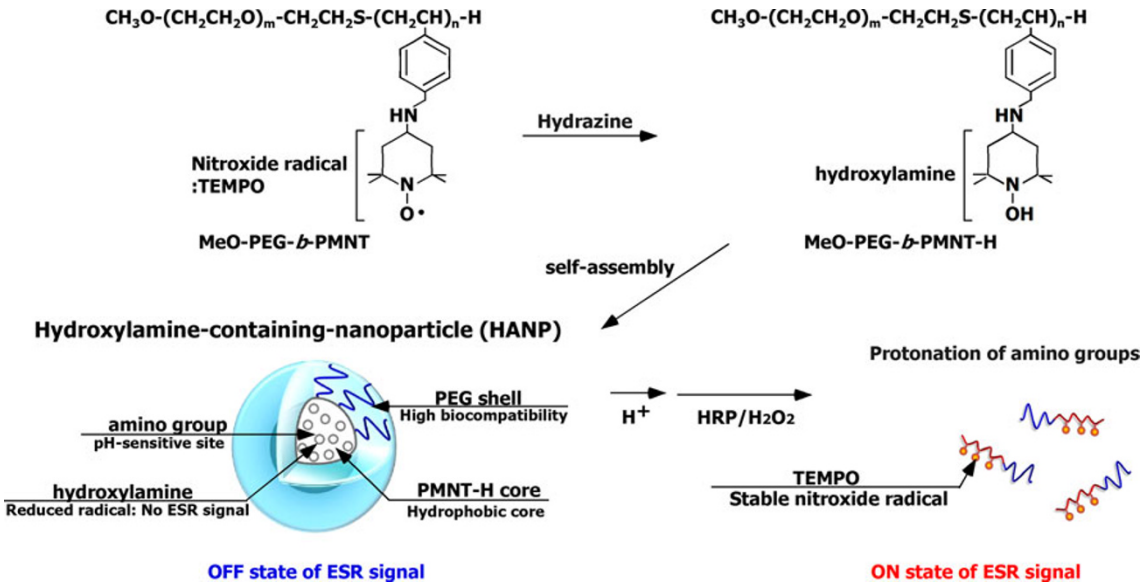

Fig. 1 Schematic illustration of HANP for inflammation sites imaging

2 Experimental Methods

2.1 Preparation of PEG-*b*-PMNT

PEG-*b*-PMNT block copolymer was prepared as previously reported [21, 22]. Briefly, MeO-PEG-*b*-poly(chloromethylstyrene) (PCMS) was synthesized by radical telomerization of chloromethylstyrene (CMS) using PEG possessing a methoxy group at the α-chain end and a sulfonyl group at the ω-chain end (MeO-PEG-SH) as a telogen. The polymer backbone of PEG-*b*-PCMS consisting of PEG with a molecular weight of 5,000 g/mol for the hydrophilic segment and 16 repeating units of PCMS for the hydrophobic segment (MW = 2,500), as determined using the ^{1}H NMR data based on the Mn of PEG. To obtain PEG-*b*-PMNT, chloromethyl groups on the PCMS segment of the block copolymer were converted to nitroxide radicals via amination of MeO-PEG-*b*-PCMS with 4-amino-TEMPO in dimethyl sulfoxide (DMSO). After purification of the obtained PEG-*b*-PMNT, the substitution ratio of the modified TEMPO moieties per repeating unit of PCMS was 80%, as determined by ESR using a standard curve generated from 4-amino-TEMPO in chloroform (MW of PEG-*b*-PMNT = 9,000).

2.2 Preparation of the HANP

The HANP was prepared from MeO-PEG-*b*-PMNT by the dialysis method in the presence of hydrazine. MeO-PEG-*b*-PMNT (4 mg, 0.44 μmol; molar quantity of nitroxide radicals = 7.04 μmol) and hydrazine anhydride (137 mg, 4.27 mmol) were dissolved in *N*,*N*-dimethylformamide (DMF) (1 mL), and the polymer solution was transferred into a membrane tube (molecular-weight cutoff size: 3,500; Spectra/Por; Spectrum, USA) and then dialyzed for 24 h against 2 L of water, which was changed after 2, 5, 8, and 20 h. Dynamic light scattering (DLS) measurements were carried out to determine the diameter of the obtained HANP after dialysis.

2.3 Synthesis of 4-Hydroxy-2,2,6,6-Tetramethylpiperidine-1-Hydroxyl (TEMPOL-H)

TEMPOL-H was prepared using a method described in a previous paper by Henry-Riyad et al. [23]. 4-Hydroxy-TEMPO (TEMPOL) (110 mg, 0.63 mmol) in an aqueous solution (1 mL) in the presence of sodium ascorbate (210 mg, 2.56 mmol) was stirred vigorously for 5 min, resulting in complete decolorization and the appearance of a white precipitate. The resulting suspension was extracted using diethyl ether, and the ether extracts were washed with water and brine, dried over anhydrous sodium sulfate, and evaporated under reduced pressure to provide TEMPOL-H (70 mg, 63%). The obtained product was used as a control after no ESR signal of TEMPOL-H was confirmed.

2.4 DLS Measurement as a Function of pH

Light scattering intensities of the pH-sensitive HANP were measured as a function of pH using a light scattering spectrometer (Nano ZS, ZEN3600, Malvern Instruments, Ltd., UK) equipped with a He–Ne laser that produces vertically polarized incident beams at a detection angle of 173° at 25°C. First, 3.5 mg/mL of the HANP solution was prepared as stock solution **A** after the formation of the HANP using a dialysis method. Britton–Robinson buffers (100 μL each) with various pH values, which were prepared from a stock solution containing 1 M phosphoric acid, 1 M boric acid, and 1 M acetic acid and by adjusting the pH value using NaOH, were added to stock solution **A** (400 μL). The mixtures with various pH values were immediately transferred to the cells and measured using DLS.

2.5 Reaction of HANP with HRP/H_2O_2 Mixture

HRP and H_2O_2 were used as models of in vivo oxidants. HANP solution (23 μg/mL, 2.3 μM) was prepared as stock solution **B** after formation of HANP using a dialysis method in the presence of hydrazine. H_2O_2 solution (500 mM, 30 μL) and HRP solution (375 U/mL, 240 μL) in 100 mM Britton–Robinson buffers at pH 5.6 or 7.4 were added to stock solution **B** (30 μL). After HANP was mixed with HRP/H_2O_2 mixture, the samples were immediately transferred to a capillary tube and measured using ESR. The TEMPOL-H solution (46 mM) was used as a control to confirm the enzymatic activity of HRP.

2.6 ESR Measurements

The ESR spectra were recorded at room temperature using a Bruker EMX-T ESR spectrometer operating at 9.7 GHz with a 100-kHz magnetic field modulation. Spectra were collected with the following parameters: sweep width, 500 G; microwave power, 0.633 mW; receiver gain, 5.02×10^4; time constant, 5.120 ms; and conversion time, 10.240 ms.

3 Results and Discussion

3.1 Preparation and Characterization of HANP

Nitroxide radicals are known to be easily reduced by hydrazine derivatives and convert to ESR and MR-insusceptible hydroxylamine form [24]. To reduce nitroxide radicals in PEG-*b*-PMNT to the corresponding hydroxylamine

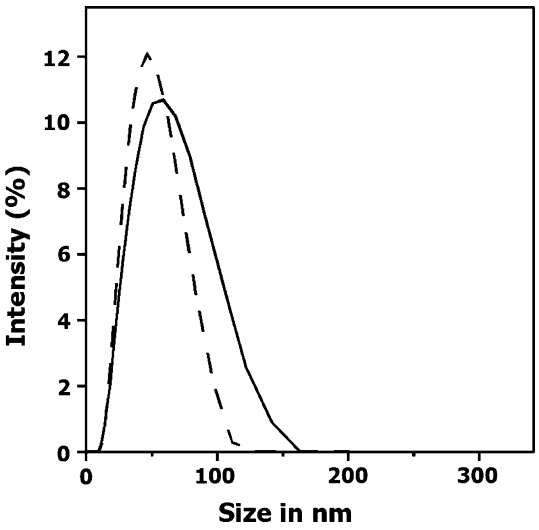

Fig. 2 Size distribution of HANP (*solid line*) and RNP (*dot line*) after dialysis

form, hydrazine was added to PEG-*b*-PMNT solution in DMF. The ESR signal of PEG-*b*-PMNT disappeared completely in DMF, indicating that the reducing reaction of nitroxide radicals in PEG-*b*-PMNT proceeded homogeneously and quantitatively (see Figure S1). To prepare HANP, the reaction mixture was dialyzed against water. Figure 2 shows the size distribution of nanoparticle prepared using dialysis with and without hydrazine, as measured by DLS. As shown in the figure, the size and distribution of nanoparticles formed in the presence or absence of reducing agent were nearly the same. The average diameter and polydispersity factor (μ_2/Γ^2) of HANP were ca. 50 nm and 0.217, respectively, as determined using the cumulant method. ESR signals of the obtained HANP and RNP were then measured at the same polymer concentration. RNP showed a broad and intense signal due to the strong spin–spin interaction because of the location of a large number of nitroxide radicals in the hydrophobic core of RNP, as shown in Fig. 3a. In contrast, HANP showed extremely small triplet ESR signals (see Fig. 3b). Evaluation of the ESR signal area indicated that 84.6% of the TEMPO radicals were reduced; thus, nearly all TEMPO radicals remain reduced in the HANP core even after dialysis. As previously reported, along with the decreasing in pH, ESR signals of RNP change from broad to sharp triplets without change in ESR signal area due to the disintegration of nanoparticle, leading to increase in the ESR signal height (see Fig. 3c) [21]. Compared to the ESR signal height of disintegrated RNP at low pH environment, the ESR signal height of HANP was only 5.7%, indicating that the background signal of HANP is extremely low.

3.2 pH Response of HANP

Polyamines with appropriate hydrophobicity, including poly[2-(*N*,*N*-diethylamino)ethyl methacrylate] (PEAMA), are known to show phase transitions as a function of pH [25–27]. Utilizing this character, various environmentally sensitive polymeric materials have been developed. For example, the swelling/deswelling behavior of a PEGylated nanogel possessing a cross-linked PEAMA core can be controlled by the environmental pH [28, 29]. In a previous study, we confirmed that RNP can disintegrate in response to low pH because the PMNT segment in PEG-*b*-PMNT possesses amino groups and a hydrophobic region in each repeating unit [21]. Similarly, HANP may disintegrate at low pH due to protonation of the amino groups in each repeating unit of the PMNT-H segment in PEG-*b*-PMNT-H. In order to confirm the disintegration of the HANP core in response to low pH, light scattering intensities of HANP solutions were measured as a function of pH. As shown in Fig. 4, the light scattering intensity of the nanoparticle prepared from PEG-*b*-PCMS (no amino groups), which is abbreviated as CNP, did not change at all, whereas it

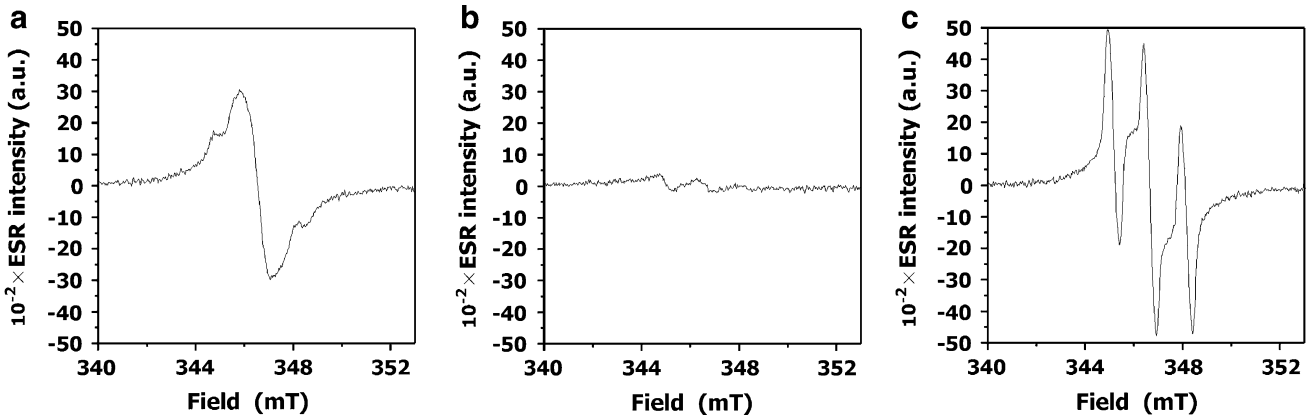

Fig. 3 ESR spectra of nitroxide radical of RNP (**a**), HANP (**b**) after dialysis and disintegrated RNP at pH 5.6 (**c**) at the same polymer concentration

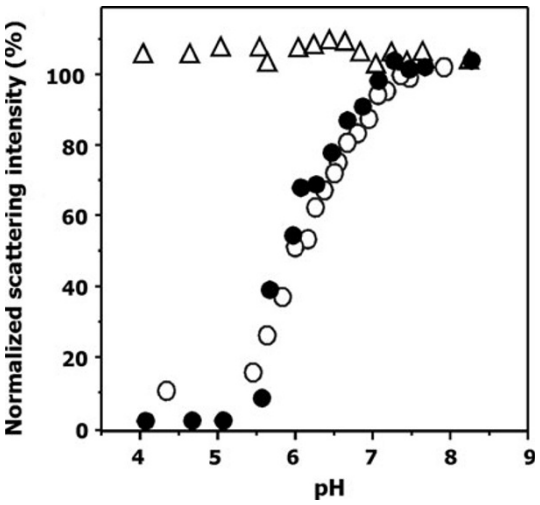

Fig. 4 Effect of pH on the light scattering intensity of HANP (*closed circle*), RNP (*open circle*) and CNP (*open triangle*). The normalized scattering intensity (%) is expressed as the value relative to that at pH 8.2

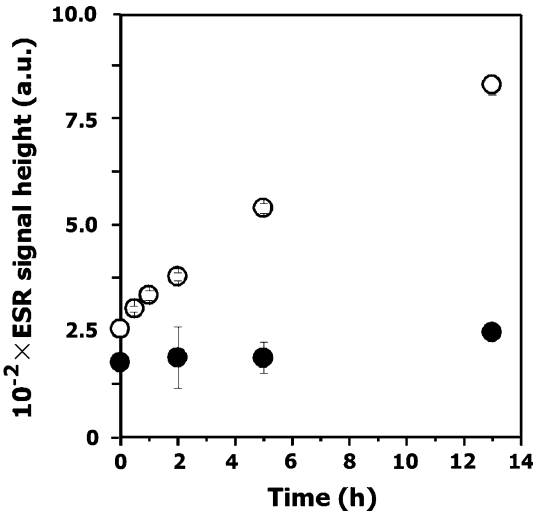

Fig. 5 Time course of ESR signal height of HANP (*closed circle*) and TEMPOL-H (*open circle*) under atmospheric conditions

drastically decreased at pH values below 7.0 in the case of HANP prepared from the PEG-*b*-PMNT-H block copolymer. According to the Rayleigh approximation [30], it is clear that the HANP disintegrated at pH values below 7.0. Because the disintegration behavior of HANP is similar to that of RNP, these results indicate that PMNT-H segments are converted from hydrophobic to hydrophilic at low pH due to protonation of the amino groups.

3.3 Detection of Oxidation Reaction Using X-Band ESR

In the imaging of inflammation sites, HANP was designed to show the following properties: (1) no signal in non-target area by the inhibiting the oxidation reaction owing to the confinement of hydroxylamine in the hydrophobic core of HANP; (2) accumulation in inflammation sites because of the increased vascular permeability; and (3) emission of an intense ESR signal in response to oxidation reaction by ROS or oxidase and low pH. However, hydroxylamine derivatives are rapidly oxidized by oxygen under atmospheric conditions; thus, its background signal gradually increases over time before use. As shown in Fig. 5, the ESR signal of low-molecular-weight TEMPOL-H in aqueous solution (pH 7.4) increased gradually. In contrast, the ESR intensity of HANP did not change at all, indicating that HANP can suppress the atmospheric oxidation reaction by oxygen due to the confinement of the hydroxylamine in the hydrophobic core of HANP.

To further investigate the pH-response of HANP in the oxidation reaction, HRP/H_2O_2 mixture was used as an in

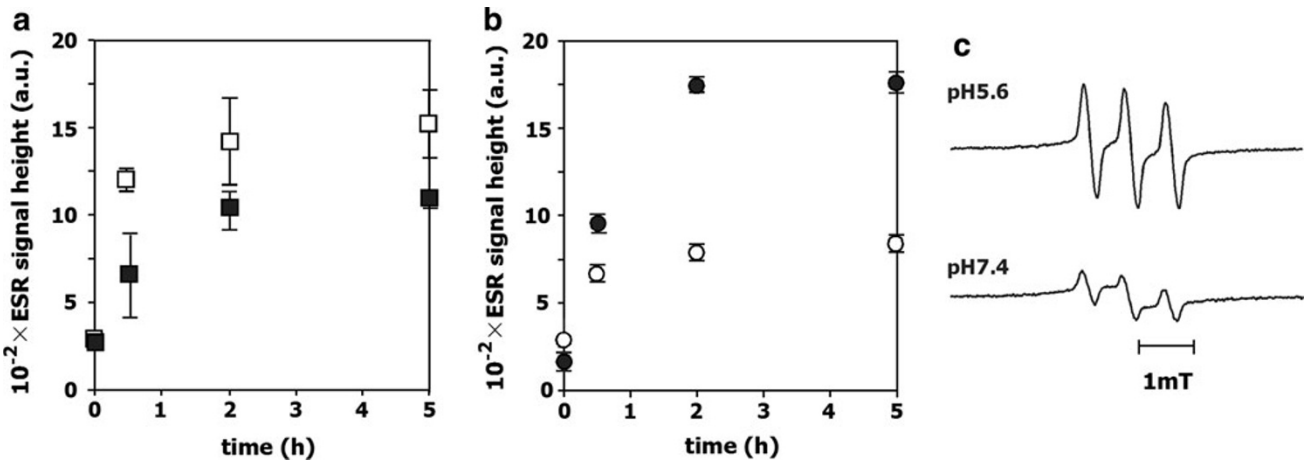

Fig. 6 **a** Time course of ESR signal height of TEMPOL-H oxidized by HRP/H_2O_2 couple at pH 5.6 (*closed square*) and pH 7.4 (*open square*). **b** Time course of ESR signal height of HANP oxidized by HRP/H_2O_2 couple at pH 5.6 (*closed circle*) and pH 7.4 (*open circle*). **c** ESR spectra of HANP at pH 5.6 and 7.4 after oxidation by HRP/H_2O_2

vivo oxidant model because the HRP/H_2O_2 mixture is known to oxidize hydroxylamine to the corresponding nitroxide radical [31]. To confirm the enzymatic activity of HRP, TEMPOL-H was mixed with the HRP/H_2O_2 mixture, followed by the ESR measurement. As shown in Fig. 6a, the ESR signal of TEMPOL-H under neutral condition (pH = 7.4) increased much faster than that under acidic condition (pH = 5.6). This result indicates that the enzymatic activity of HRP at pH 7.4 is much higher than that of HRP at pH 5.6. It is agreed well with previous report [32]. Similar to low-molecular-weight TEMPOL-H, the oxidation of hydroxylamine was observed when HANP was mixed with HRP/H_2O_2 couple. It is interesting to note that the ESR signal under acidic condition (pH = 5.6) increased much faster than that under neutral condition (pH = 7.4) (see Fig. 6b), although the enzymatic activity of HRP at neutral pH is higher than that of HRP at acidic pH, as stated above. The result means that the enzymatic oxidation reaction was accelerated by synchronizing the disintegration of HANP under acidic conditions. A significant increase in signal height was observed at pH 5.6, as shown in Fig. 6c. Because of the difference in the ESR signal height of HANP between acidic and neutral conditions, inflammation sites can be visualized using in vivo ESR imaging. Since nitroxide radical is also susceptible to nuclear magnetic resonance, this system has applicability to MR imaging.

4 Conclusion

In this paper, the design and preparation of an ESR nanoprobe for imaging inflammation sites are described. This nanoprobe is based on a pH-sensitive hydroxylamine-containing-nanoparticle (HANP) consisting of a PEG-*b*-PMNT-H block copolymer. Disintegration of HANP was observed at pH values below 7.0; this change was caused by protonation of amino groups on the PMNT-H segments in response to the acidic pH environment. HANP shows not only suppression of atmospheric oxidation reaction by oxygen, but also the ability of on–off regulation of the ESR signal in response to low pH and enzymatic oxidation reaction. Based on these results, pH-sensitive HANP is anticipated as high-performance nanoprobe for inflammation sites imaging.

Acknowledgments A part of this work was supported by Grant-in-Aid for Scientific Research A (21240050) and Grant-in-Aid for Research Activity Start-up (22800004) and the World Premier International Research Center Initiative (WPI Initiative) on Materials Nanoarchitronics of the Ministry of Education, Culture, Sports, Science and Technology (MEXT) of Japan.

References

1. Ulbrich W, Lamprecht A (2010) J R Soc Interface 7:S55
2. Weitzman SA, Gordon LI (1990) Blood 76:655
3. Coussens LM, Werb Z (2002) Nature 420:860
4. Maeda H, Fang J, Inutsuka T, Kitamoto Y (2003) Int Immunopharmacol 3:319
5. Lamprecht A, Schafer U, Lehr C-M (2001) Pharm Res 18:788
6. Bryant RE, Rashad AL, Mazza JA, Hammond D (1980) J Infect Dis 142:594
7. Simmen HP, Battaglia H, Giovanoli P, Blaser J (1994) Infection 22:386
8. Martínez D, Vermeulen M, Trevani A, Ceballos A, Sabatté J, Gamberale R, Álvarez ME, Salamone G, Tanos T, Coso OA, Geffner J (2006) J Immunol 176:1163
9. Berliner LJ, Khramtsov V, Fujii H, TL Clanton (2001) Free Radic Biol Med 30:489
10. Inbaraj JJ, Cardon TB, Laryukhin M, Grosser SM, Lorigan GA (2006) J Am Chem Soc 128:9549
11. He G, Deng Y, Li H, Kuppusamy P, Zweier JL (2002) Magn Reson Med 47:571
12. Soule BP, Hyodo F, Matsumoto K, Simone NL, Cook JA, Krishna MC, Mitchell JB (2007) Free Radic Biol Med 42:1632
13. Rosen GM, Finkelstein E, Rauckman EJ (1982) Arch Biochem Biophys 215:367
14. Nilsson UA, Olsson LI, Thor H, Moldeus P (1989) Free Radic Biol Med 6:251
15. Dikalov S, Skatchkov M, Bassenge E (1997) Biochem Biophys Res Commun 230:54
16. Marushima A, Suzuki K, Nagasaki Y, Yoshitomi T, Toh K, Tsurushima H, Hirayama A, Matsumura A (2011) Neurosurgery 68:1418
17. Yoshitomi T, Hirayama A, Nagasaki Y (2011) Biomaterials 32:8021
18. Chonpathompikunlert P, Yoshitomi T, Han J, Toh K, Isoda H, Nagasaki Y (2011) Ther Deliv 2:585
19. Chonpathompikunlert P, Yoshitomi T, Han J, Isoda H, Nagasaki Y (2011) Biomaterials 32:8605
20. Yoshitomi T, Nagasaki Y (2011) Nanomedicine 6:509
21. Yoshitomi T, Suzuki R, Mamiya T, Matsui H, Hirayama A, Nagasaki Y (2009) Bioconjugate Chem 20:1792
22. Yoshitomi T, Miyamoto D, Nagasaki Y (2009) Biomacromolecules 10:596
23. Henry-Riyad H, Tidwell TT (2003) J Phys Org Chem 16:559
24. Yoshida E, Tanaka T (2006) Colloid Polym Sci 285:135
25. Lee AS, Gast AP, Butun V, Armes SP (1999) Macromolecules 32:4302
26. Addison T, Cayre OJ, Biggs S, Armes SP, York D (2008) Langmuir 24:13328
27. Asayama S, Maruyama A, Cho C, Akaike T (1997) Bioconjugate Chem 8:833
28. Hayashi H, Iijima M, Kataoka K, Nagasaki Y (2004) Macromolecules 37:5389
29. Oishi M, Nagasaki Y (2007) React Funct Polym 67:1311
30. Huh KM, Min HS, Lee SC, Lee HJ, Kim S, Park K (2008) J Control Release 126:122
31. Utsumi H, Yamada K, Ichikawa K, Sakai K, Kinoshita Y, Matsumoto S, Nagai M (2006) Proc Natl Acad Sci USA 103:1463
32. Aoyama M, Shiga M, Ohya H, Kamada H (1998) Anal Sci 14:1107